NUMERICAL METHODS USED IN AEROELASTICITY SIMULATIONS

Serge Piperno
CERMICS
INRIA
06902 Sophia-Antipolis Cedex
France

Abstract

In this paper, we survey numerical methods used in aeroelasticity simulations. These methods are based on two-dimensional Euler equations. However, they are quite general. First, we consider fluid dynamics numerical methods, which are also used to solve moving boundaries problems. Fixed computational domain methods (possibly with multiple moving frames of reference) are introduced. Arbitrary Lagrangian-Eulerian and dynamic meshes formulations are also presented. Second, we discuss the most used algorithm for interaction simulation in aeroelastic computations. Finally, we present numerical methods for structural dynamics.

QUELQUES METHODES NUMERIQUES UTILISEES EN AEROELASTICITE

Résumé

Dans ce rapport, nous présentons un éventail de méthodes numériques pour l' aéroélasticité. Ces méthodes s'adaptent à de nombreux types d'équations. Elles sont ici exposées sur la base des équations d'Euler bi-dimensionnelles. Dans un premier temps, nous considérons les méthodes utilisées pour la partie fluide, qui permettent aussi de résoudre des problèmes à parois mobiles. Nous présentons des méthodes à domaine de calcul fixe, avec d'éventuels repères mobiles, ainsi que les formulations de type ALE ou maillages dynamiques. Ensuite, nous analysons l'algorithme généralement utilisé pour simuler l'interaction. Enfin, nous présentons quelques méthodes numériques pour simuler les mouvements des structures.

1 Introduction

Aeroelastic phenomena are particular cases of fluid-structure interactions. In aeroelasticity, an external or internal flow and an elastic deforming structure are submitted to forces or physical actions from one another. The pressure of the fluid is exerted on the shape of the structure and the structure enforces boundary conditions to the flow. These boundary conditions along the fluid-structure interface are enforced in location and speed by the structure.

Years ago, arerodynamics specialists turned their investigations towards moving boundaries problems. Another step was made when the first aeroelasticians studied new fluid-structure interactions. In those cases, the motions of the boundary conditions were no longer a priori decided, but flow dependent. The coupling phenomena between the fluids and the structures were about to be numerically simulated and investigated.

This kind of computations was first necessary for safety studies on heavy structures submitted to a certain flow. They were not only aeroelastic simulations but also hydroelastic (cases where the fluid is rather heavy and incompressible like liquids : sea water, liquid sodium, etc...). For example, lots of computations were performed for Nuclear Reactor Safety studies. In [7], the authors give many references to hydroelastic computational efforts. For this kind of problems, the question was : in which way can a nuclear structure react under an internal explosion, shock waves or periodic excitations from the fluid. This last problem was met in the French "surregenerateur" Super-Phenix in which a periodic mode had been observed with a threatening amplitude (outflow of liquid sodium between a thin, deforming vessel and a thicker external one). Structural fatigue was also studied for motions of non-negligible amplitude. Other hydroelastic calculations were performed for objects like submarines, which can meet explosions and shock-waves produced by depth-charges. Other cases could be considered, such as motions and acoustics in pipes.

Another kind of computations were performed mainly in an aeroelastic framework in order to study and understand instabilities in flows when they are coupled with a structure. For example, lots of structural dynamists and civil engineers have brooded over the case of the original Tacoma Narrows bridge and its famous failure. In [27], Scanlan surveys the 1979 state of the art on the three outstanding problems of suspended-span bridges in wind, namely vortex shedding, flutter and buffeting. In figure 1, we can understand how torsional flutter can find its origin in an evolution of aerodynamic damping towards negative values as wind velocity increases. Rotation of the leading surface upward is accompanied with vortices displacements which give rise to locally destabilizing pressures (tending to increase the motion that created them).

In aeronautics, flutter phenomena have been much studied. Lots of aeroelastic computations were produced on the solution of the very well known transonic dip [8]. The aeroelastic coupling was also used to enhance the performances of modern planes. These more and more flexible structures need a very efficient limitation of aeroelastic interactions with active control surfaces. These control surfaces were introduced for example in [13] and improved in [10].

In this bibliographical report, we survey the numerical methods which are most commonly used in aeroelastic simulations. These methods are generally applicable to other fluid-structure interaction simulations, like hydroelastic cases. We will discuss neither the model equations used for the flow nor the complexity of the geometry under consideration (a typical wing

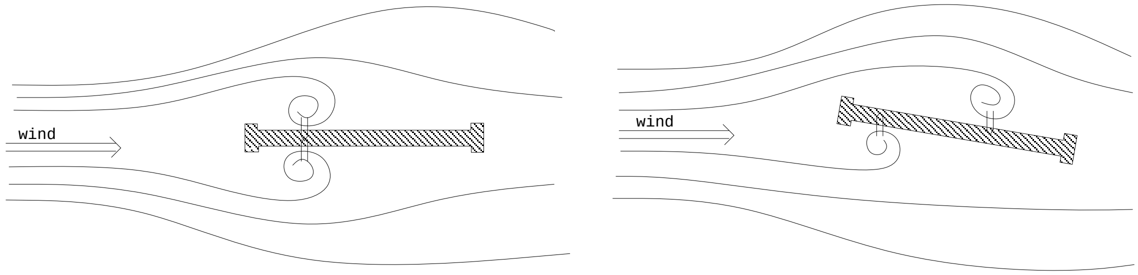

Figure 1: vortices around a bridge in torsional motion.

profile, a wing-body configuration, a complete airfoil...). A summary and a brief chronology of the development of advanced computational fluid dynamics techniques and their application to aeroelasticity can be found in [8].

In the following, we will use the two-dimensional Euler equations for the fluid. The methods presented are consistent with any other model equations (like Full Potential equations or Navier-Stokes equations). As we just stated, the integration of a phenomenon with aeroelastic coupling can be achieved if we can perform integrations of both model equations for the fluid and the structure at the same (computational and physical) time. In this paper, we will first present in Section 2 numerical methods for flow simulations which have been created or adapted to aeroelastic cases. They are identical with numerical methods for moving boundaries problems. We will then study in Section 3 the general algorithm for a simultaneous integration of reciprocal actions of the fluid and the structure on one another. At last, we will present numerical methods for the resolution of structural dynamics in Section 4.

2 Numerical methods for flow simulations.

In this section, we consider the fluid part of the problem. The flow evolves in a moving boundary domain and we suppose that the movement of these boundaries is already known. All methods presented here are adaptable or used in pure time-dependent domain problems.

Since the location of the structure changes, the spatial discretization – a structured or unstructured mesh – has to be calculated and updated after (or before) each time step, or at least after every significant move of the structure.

However, there are cases where these grid calculations can be limited or simply eliminated. For example, if one simulates the two-dimensional gas flow around a rigid wing profile, one can write the whole set of equations of your physical model in a moving body-fixed frame of reference. The motivation of the different methods used for the flow simulation lies in the simplifications of the equations or of the CPU expensive grid computation phases. Most of the following procedures have features which are real advantages in very specific configurations.

The sequel of the section is dealing first with basic fixed computational domain methods and then with fixed computational domain methods with moving frames of reference. Thereafter, the class of methods based on pure Arbitrary Lagrangian-Eulerian formulation is presented, and this flow-devoted section will be concluded with the dynamic meshes methods, which are not very different from ALE methods, excepted that they can be made consistent with global upwind schemes.

2.1 Fixed computational domain methods.

Let us consider the case of the numerical simulation of a two-dimensional flow around a wing profile. The wing is likely to move and/or warp. Therefore, the grid used for the spatial discretization will have to be updated. Since the grid moves, spatial derivatives in Euler equations will need higher cost computations.

It is generally preferred to use a structured body-conforming grid (for example, a O-mesh or a C-mesh around a profile), which is perfectly regular in the space of body-fitted coordinates. If the body moves, the grid may change, but the indices of the cells in the structured grid will remain fixed. The computational domain of cell indices is fixed and the transformation Jacobian from the computational domain to the physical domain is varying. Thereby, it is much simpler to write the model equations in body-fitted coordinates. The computations of all body-fitted derivatives will be very cheap since the fixed computational domain (FCD) is uniformly grided. In the following, the curvilinear body-fitted coordinates will be ξ and η. For example, the case of a flow around a wing profile is shown on figure 2. The curvilinear body-fitted coordinate ξ is taken around the wing and η normal to the wing.

Formulation (see e.g. [9]) :

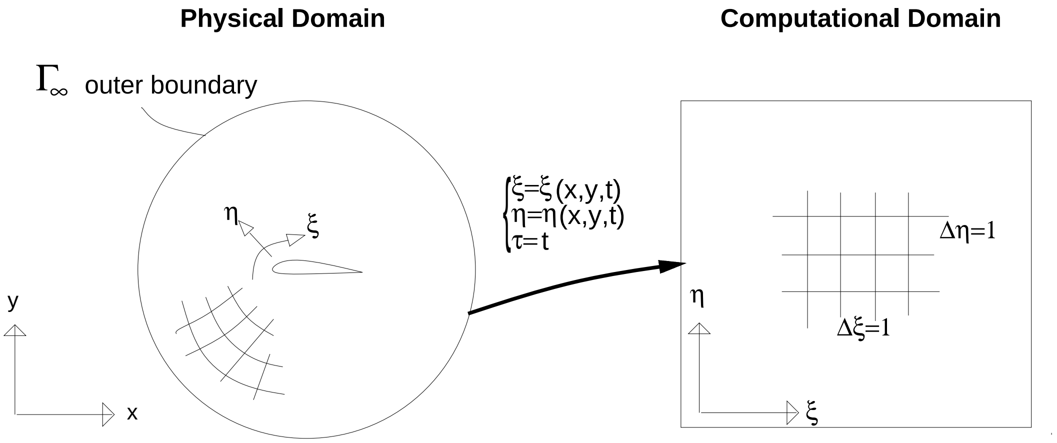

Figure 2: body-fitted curvilinear coordinates transformation.

- The first step to obtain the formulation consists in moving from the Cartesian coordinates to the curvilinear coordinates using

$$\left\{ \begin{array}{lcl} \tau & = & t \\ \xi & = & \xi(x, y, t) \\ \eta & = & \eta(x, y, t). \end{array} \right. \tag{1}$$

- The transformation is chosen in order to handle near and farfield fluid boundary conditions very easily. For an O-mesh, the shape of the structure would be defined by $\eta = \eta_0$ and the farfield fluid boundary by $\eta = \eta_\infty$.

- The two-dimensional Euler equations for an ideal gas in Cartesian coordinates may be written as

$$\boxed{\frac{\partial Q}{\partial t} + \frac{\partial E}{\partial x} + \frac{\partial F}{\partial y} = 0} \tag{2}$$

where

$$Q = \begin{pmatrix} \rho \\ \rho u \\ \rho v \\ e \end{pmatrix}, \qquad E = \begin{pmatrix} \rho u \\ \rho u^2 + p \\ \rho u v \\ (e + p)u \end{pmatrix}, \qquad F = \begin{pmatrix} \rho v \\ \rho u v \\ \rho v^2 + p \\ (e + p)v \end{pmatrix}, \tag{3}$$

where ρ, u, v, e and p are respectively the density, the projected gas velocities along Cartesian axes, the volumic energy and the pressure given by

$$p = (\gamma - 1)[e - \frac{1}{2}\rho(u^2 + v^2)]. \tag{4}$$

- These equations are transformed when expressed in curvilinear coordinates and they now take the form

$$\boxed{\frac{\partial \hat{Q}}{\partial \tau} + \frac{\partial \hat{E}}{\partial \xi} + \frac{\partial \hat{F}}{\partial \eta} = 0} \tag{5}$$

where the transformed quantities wear a ' ^ ' and

$$\hat{Q} = J^{-1} \begin{pmatrix} \rho \\ \rho u \\ \rho v \\ e \end{pmatrix},$$
$$\hat{E} = J^{-1} \begin{pmatrix} \rho U \\ \rho u U + \xi_x p \\ \rho v U + \xi_y p \\ (e+p)U - \xi_t p \end{pmatrix}, \qquad \hat{F} = J^{-1} \begin{pmatrix} \rho V \\ \rho u V + \eta_x p \\ \rho v V + \eta_y p \\ (e+p)V - \eta_t p \end{pmatrix}, \tag{6}$$

where for instance the notation 'ξ_x' stands for $\partial\xi/\partial x$, J is the determinant of the transformation to curvilinear coordinates defined by (1), i.ei :

$$J = \begin{vmatrix} \xi_x & \xi_y & \xi_t \\ \eta_x & \eta_y & \eta_t \\ 0 & 0 & 1 \end{vmatrix} = \xi_x \eta_y - \xi_y \eta_x \tag{7}$$

and where U and V are contravariant velocity components defined as

$$\begin{cases} U = \xi_t + \xi_x u + \xi_y v \\ V = \eta_t + \eta_x u + \eta_y v. \end{cases} \tag{8}$$

The uniform grid of the fixed computational domain has unit steps in all directions ($\Delta\xi = 1, \Delta\eta = 1$). Since the grid is structured, the derivatives of any quantity w according to the curvilinear coordinates ξ, η may be computed by $w_\xi = w(\xi_{n+1}) - w(\xi_n)$, etc ... The Cartesian derivatives of w are easily expressed with curvilivear derivatives with relations such as

$$w_x = \xi_x w_\xi + \eta_x w_\eta. \tag{9}$$

The cartesian derivatives of curvilinear coordinates appearing in (6), (8) or (9) can be obtained via chain-rule expansions stemming from

$$\begin{pmatrix} \xi_x & \xi_y & \xi_t \\ \eta_x & \eta_y & \eta_t \\ 0 & 0 & 1 \end{pmatrix} \begin{pmatrix} x_\xi & x_\eta & x_\tau \\ y_\xi & y_\eta & y_\tau \\ 0 & 0 & 1 \end{pmatrix} = \begin{pmatrix} 1 & 0 & 0 \\ 0 & 1 & 0 \\ 0 & 0 & 1 \end{pmatrix} \tag{10}$$

which give after simplifications

$$\begin{array}{llll} \xi_x & = J y_\eta & \eta_x & = -J y_\xi \\ \xi_y & = -J x_\eta & \eta_y & = J x_\xi \\ \xi_t & = -x_\tau \xi_x - y_\tau \xi_y & \eta_t & = -x_\tau \eta_x - y_\tau \eta_y. \end{array} \tag{11}$$

• The equations (2) and (5) have identical characteristics (they are both hyperbolic systems of conservation laws) and several numerical schemes for the transformed equations have been developed from classical Euler solvers. For example, Van Leer flux decomposition for curvilinear coordinates can be found in [1] and streamwise flux vector splittings and Roe's approximate Riemann solver are written in [24]. It is also possible to obtain similar equations for three-dimensional problems. The complete set of equations for the fluid and the geometric variables can be found in [9]. The global algorithm is now described.

Algorithm :

- At the current step of the numerical simulation, we suppose that we know at time level t_n the following quantities :

  - all geometric quantities on the whole grid, like the functions $x = x(\xi, \eta, t_n)$, $y = y(\xi, \eta, t_n)$ and the derivatives x_ξ, x_η, y_ξ, y_η,
  - the grid speeds x_τ and y_τ,
  - the transformed vector of conserved variables $\hat{Q}$.

- The system (5) is integrated from time level t_n to $t_{n+1} = t_n + \delta t_n$ with fixed geometric quantities. The boundary conditions for this integration are translated from the physical ones (no normal speed along the surface of the structure boundary and fixed values on the farfield fluid boundary).

- All geometric quantities must then be updated to evaluate them at time level t_{n+1}. There are many different routines for this last phase.

In a first family, the boundary points are first updated (according to the known motion of the boundaries) and, in a second step, the locations of interior points are deduced with several methods. Guruswamy has introduced in [9] an algebraic grid regeneration formula for a complete three-dimensional wing. Batina used in [2] an adaptation method based on springs analogy. Nakahashi and Deiwert presented in [22] variational principles with smoothness and orthogonality constraints for the generation of the new interior grid. At the end of this step, all purely geometric quantities should be computed and the grid speeds updating scheme takes the following finite difference form :

$$x_\tau^{n+1} = \frac{x^{n+1} - x^n}{\delta t_n} \quad \text{and} \quad y_\tau^{n+1} = \frac{y^{n+1} - y^n}{\delta t_n}. \tag{12}$$

In a second family of grid updating methods, the new locations of all interior points are deduced from their previous location and their previous grid speed according to

$$x^{n+1} = x^n + \delta t_n . x_\tau^n \quad \text{and} \quad y^{n+1} = y^n + \delta t_n . y_\tau^n. \tag{13}$$

During the second step, new grid speeds must be generated. Shankar and Ide have presented in [28] such a scheme with linear interpolation from the structure to the fixed farfield fluid boundary along "$\xi = \xi_0$" lines.

Both types of methods are nearly equivalent. Their qualitative difference is induced by the different roles played by the grid speeds in (12) and (13).

Drawbacks and limits.

- The original Euler equations have become much more complex but the resolution of the new equations is more efficient.

- Difficulties may appear in the cases of important deformations and/or large motions. The updating schemes we just reviewed have no theoretical generality.

- These methods strongly use the fact that the grid is structured. Extension to body-fitted coordinates with unstructured meshes seems uneasy. Even if this extension could be done, the computational time used for spatial derivatives calculations would reduce the efficiency of the method.

- Numerical unstabilities may appear with the use of auxiliary geometric time-dependent variables such as cell-volums, transformation Jacobians – like J^{-1} in (5). There exists a geometric conservation law, described by Thomas and Lombard in [29], which is deriving from the following principle : the volume of a portion of physical space does not depend on the space discretization. This law can be written as

$$\boxed{\frac{\partial J^{-1}}{\partial \tau} + \frac{\partial (J^{-1}\xi_t)}{\partial \xi} + \frac{\partial (J^{-1}\eta_t)}{\partial \eta} = 0.} \tag{14}$$

After a time step, it would be dangerous to update the Jacobian J of the transformation at the cell (i, j) of the structured grid according to

$$\begin{aligned} 2\Delta\xi\Delta\eta J^{-1} \;\; = \;\; & [(x_{i+1,j} - x_{i,j})(y_{i+1,j+1} - y_{i,j+1}) \\ & -(x_{i+1,j+1} - x_{i,j+1})(y_{i+1,j} - y_{i,j})] \end{aligned} \tag{15}$$

(we remind that $\Delta\xi = \Delta\eta = 1$) or to anything else but a scalar version of the time-integration scheme used for (5).

- For all the fixed computational domain methods presented heretofore, all geometric variables, the grid, the spatial and temporal Jacobians fields, have to be regenerated and updated. These CPU expensive phases of the algorithm are run without searching any possibility of global simplification, as for a simple rigid-body motion. This is precisely why methods with moving frames of reference have been developed.

2.2 FCD methods with moving frames of reference.

The need for moving frames of reference appeared in the study of particular flows around a structure. The algorithm presented in the previous section is in some sense the algorithm of the worst case. The structure is moving and may be deforming, so heavy grid computations are necessary after each time step to be ready for every emergency. This blind policy is certainly inefficient in cases where global simplifications or CPU savings are possible.

For example, Kandil and Chuang presented in [14] a numerical simulation of a two-dimensional flow around a rigid moving wing-profile. In a wing-linked frame of reference, different from the laboratory frame of reference, the wing is obviously rigid and fixed. In this frame of reference, the original grid – and geometric quantities – can be used during the whole time-integration. We just need a new formulation of our physical problem in a moving frame of reference.

Formulation (see e.g. [9]) : **Formulation** (see [18]) :

• The classical Euler equations (2) and (3) are rewritten in a frame of reference different from the frame linked to the laboratory. There may coexist several frames of reference. The j^{th} time-dependent frame is defined by :

- ∘ $\vec{r_j}$: position of the origin,
- ∘ T_j : set of direct orthonormal axes directions,
- ∘ $\vec{v_j} = d\vec{r_j}/dt$ and $\vec{a_j} = d\vec{v_j}/dt$: velocity and acceleration of the moving frame,
- ∘ $\vec{\omega_j}$ and $\dot{\vec{\omega_j}} = d\vec{\omega_j}/dt$: angular velocity and acceleration of the moving frame.

We want to translate Euler equations in multiple moving frames of reference. We have to recall that spatial derivatives in Euler equations will induce spatial derivatives of new conservative variables for the fluid and also spatial derivatives of the definitions elements of the frames of reference, since the frame considered depends on the location in the frame of the laboratory. Euler equations take the form :

$$\boxed{\frac{\partial Q'}{\partial t} + \frac{\partial E'}{\partial x'} + \frac{\partial F'}{\partial y'} = S'} \tag{16}$$

where

$$Q' = \begin{pmatrix} \rho \\ \rho u' \\ \rho v' \\ e' \end{pmatrix}, \quad E' = \begin{pmatrix} \rho u' \\ \rho u'^2 + p \\ \rho u'v' \\ (e'+p)'u \end{pmatrix}, \quad F' = \begin{pmatrix} \rho v' \\ \rho u'v' \\ \rho v'^2 + p \\ (e'+p)v' \end{pmatrix} \tag{17}$$

and where

$$\begin{aligned}
S' &= (S'_1, S'_2, S'_3, S'_4)^t \\
S'_1 &= -\rho div(\vec{V_t}) \\
S'_2 &= -\rho a_{tx'} - \rho.div(\vec{V_t}).u' \\
S'_3 &= -\rho a_{ty'} - \rho.div(\vec{V_t}).v' \\
S'_4 &= -\rho\vec{V}.(\vec{a_t} - \vec{\omega_j} \times \vec{V'}) - (e'+p)div(\vec{V_t}) \\
\vec{r'} &= \text{ position of the point with respect to the moving frame} \\
\vec{V'} &= (u',v')^t \text{ in the moving frame of reference} \\
\vec{V} &= (u,v)^t \text{ in the absolute frame of reference} \\
\vec{V_t} &= \vec{v_j} + \vec{\omega_j} \times \vec{r'} \\
\vec{V'} &= \vec{V} - \vec{V_t} \\
e' &= e + \rho\vec{V}.\vec{V_t} \\
\vec{a_t} &= \vec{a_j} + \dot{\vec{\omega_j}} \times \vec{r'} + \vec{\omega_j} \times (\vec{\omega_j} \times \vec{r'}) + 2\vec{\omega_j} \times \vec{V'}.
\end{aligned} \tag{18}$$

In the preceding equations, the temporal derivative $\partial/\partial t$ means a differentiation with respect to the time with the moving frame of reference coordinates (x', y') held constant. The divergence term $div\vec{V}_t$ represents the influence of the variation of the transformation velocity with the physical point. We could think that $div\vec{V}_t = 0$ because of the form of $\vec{V}_t$. But we must recall that the frame of reference a physical point is referred to depends on this point. Thus, the term $div\vec{V}_t$ includes derivatives of the quantities defining the reference frames with respect to the spatial coordinates.

These equations are valid if all variables (speeds, vector components, basis directions (x', y'), etc...) are taken in the same frame of reference. The divergence terms do not depend of the frame considered since for any vector field $\vec{K}$ we have

$$\begin{gathered} \vec{K} = K_x\vec{x} + K_y\vec{y} = K_{x'}\vec{x'} + K_{y'}\vec{y'} \\ \Downarrow \\ \frac{\partial K_x}{\partial x} + \frac{\partial K_y}{\partial y} = div_{\vec{x}}(\vec{K}) = div_{\vec{x}'}(\vec{K}) = \frac{\partial K_{x'}}{\partial x'} + \frac{\partial K_{y'}}{\partial y'}. \end{gathered} \tag{19}$$

• From the preceding intermediate formulation, it is now possible to use again a transformation to curvilinear body-fitted coordinates. Since the equations (16) and (17) are already very heavy, the relative cost of the transformation is reduced. The new mapping is given by :

$$\left\{ \begin{array}{lcl} \tau & = & t \\ \xi' & = & \xi'(x', y', t) \\ \eta' & = & \eta'(x', y', t). \end{array} \right. \tag{20}$$

and the curvilinear transformation leads to

$$\boxed{\frac{\partial \hat{Q}'}{\partial \tau} + \frac{\partial \hat{E}'}{\partial \xi'} + \frac{\partial \hat{F}'}{\partial \eta'} = \hat{S}'} \tag{21}$$

where

$$\hat{S}' = J'^{-1}S' \tag{22}$$

and $\hat{Q}'$, $\hat{E}'$, $\hat{F}'$ and J' are given by equations similar to (6), (7), (8) and (11), written with the quotted variables u', v', e', U', V', ξ', η', x', y'.

Algorithm :

• The algorithm is very similar to the previous one. Before a time step, we dispose of the vector field $\hat{Q}'$, the geometric mappings $x' = x'(\xi', \eta', \tau)$, $y' = y'(\xi', \eta', \tau)$, and their derivatives $x'_{\xi'}$, $x'_{\eta'}$, $y'_{\xi'}$, $y'_{\eta'}$, x'_τ and y'_τ. We have also stored the definitions of the moving frames of reference (i.e. $\vec{r_j}$, T_j, $\vec{V_j}$, $\vec{a_j}$, $\vec{\omega_j}$, $\dot{\vec{\omega_j}}$) and for each point of the grid, the index of the frame of reference in which it is considered.

• The system (21) is integrated from time level t^n to $t^{n+1} = t^n + \delta t^n$ with the preceding geometric quantities. The boundary conditions are translated in the corresponding frame of reference.

• All geometric quantities are updated with equations corresponding to (12) and (13). The characteristics of the moving frames of reference need also an updating scheme. The moving frames are very often linked to positions of structural elements, for example the center of gravity and the chord of a rigid two-dimensional wing-profile. As soon as all geometric variables are updated, the definition elements $\vec{r_j}$, T_j, $\vec{V_j}$, $\vec{\omega_j}$ are easily deduced. The translational accelerations $\vec{a_j}$ (and of course the angular acceleration $\dot{\vec{\omega_j}}$) can be updated with formulas such as

$$\begin{aligned} \vec{a_j}^{n+1} &= \frac{1}{\delta t^n}(\vec{V_j}^{n+1} - \vec{V_j}^n) \quad \text{(first-order accurate)} && (23) \\ \text{or :} \quad \vec{a_j}^{n+1} &= \frac{2}{\delta t^n}(\vec{V_j}^{n+1} - \vec{V_j}^n) - \vec{a_j}^n \quad \text{(second-order accurate).} && (24) \end{aligned}$$

Advantages of these methods :

Up to now, the advantages of fixed computational domain methods with moving frames of reference are mostly hidden behind the drawbacks we listed in the previous section and the additional complexity due to multiple moving frames of reference. The savings and the updating schemes for the characteristics of the moving frames also increase the computational total cost. However, we show in the following particular cases where strong advantages appear.

The first category of favourable cases we consider regroups rigid-body motions of structures in an external flow. We find in this class the case presented by Kandil and Chuang in [14] but no cases with one fixed and one moving structure at the same time, like the cases of an object falling into supersonic free stream under a wing or a shock-box interaction near a wall presented by Löhner in [19]. For these cases, it is not possible to keep the same grid along the whole computation with one single moving frame of reference linked with the moving structure, since the boundaries move in this frame. On the contrary, for a rigid-body moving wing-profile, no grid updating computation is needed with a single frame of reference attached to the wing. In this case, it is worth noticing that the source term $\hat{S}'$ in (21) is a little lightened since $div(\vec{V_t}) = 0$.

A second family of applications is formed by cases of a flexible structure undergoing light elastic deformations. Due to the small changes of the shape, the grid and the spatial metrics have to be updated. In [18], Lin demonstrated that the actual positions of the grid points are not necessary for the resolution of (21), and showed an approximate spatial metrics updating scheme for the case of a flexible wind-profile in an external flow. This fast updating scheme is strongly related to multiple moving frames of reference. There is actually one frame for each $\xi = \xi_j$ line of the grid. Each frame has the orientation of the wing chord and for origin the point with curvilinear coordinates equal to (ξ_j, η_0) (see figure 3). The main idea of the scheme is to deduce variations of the metrics on the whole grid from the corresponding variations along the shape of the structure, which themselves are deduced from the deformations of the elastic structure (see [17] for more details). This formulation is particularly well suited to the physical problem under consideration, since every specific feature of the problem is taken into account in order to speed up the resolution : body-fitted coordinates, only farfield fluid boundaries, moving frames of reference corotational with the chord of the elastic wing-profile (with small deformations).

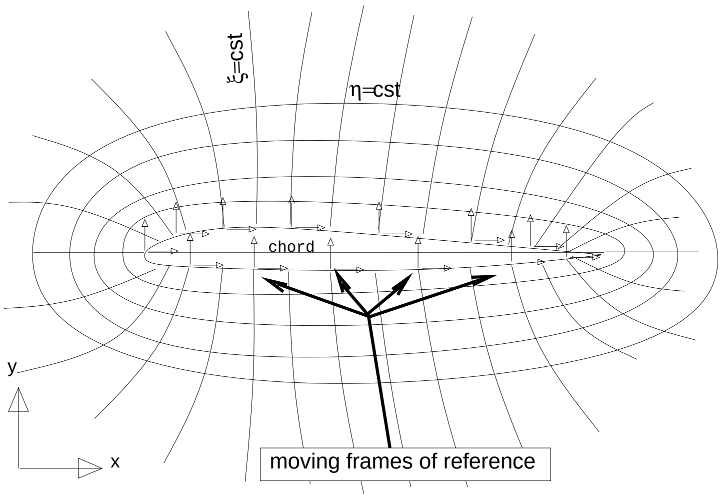

Figure 3: wing linked multiple moving frames of reference.

Though these methods allow consequent savings in computation time and memory, they are not really general, i.e. the fast metrics updating scheme must be adapted to each simulation. Furthermore, two secondary drawbacks are still persisting. First, difficulties may arise for large and/or rapid deformations. Second, the use of body-fitted curvilinear coordinates requires structured meshes, which are seldom available for cases such as complex aircraft configurations.

In methods with fixed computational domain, we considered cells fixed in the non-physical computational domain. Each cell represented in a certain way a part of the physical space. Since we had to deal with this given representation, we used structured meshes for simplification. We can now imagine methods where physical cells are considered. In such methods, like Arbitrary Lagrangian-Eulerian methods or methods using dynamic meshes we will now present, the form of the cells can be chosen freely and we will be able to use unstructured meshes.

2.3 Arbitrary Lagrangian Eulerian methods.

The Arbitrary Lagrangian Eulerian formulation (ALE) [7] has been constructed in order to avoid the shortcomings of both purely Lagrangian and Eulerian formulations and to gather all their advantages. On the one hand, the Lagrangian approach was employed with good efficiency in hydro-structural problems [6] for the kinematic description of the fluid domain. However, its ability to follow strong distorsions in complex flows is very limited. On the other hand, the Eulerian formulation easily deals with complex strongly distorted flows, but treats with less accuracy interface definitions and fluid-structure coupling.

The basic principle of ALE formulations consists in having an hybrid point of view on the flow. In a purely Eulerian study, our point of view is fixed in the physical laboratory and we study at each point physical variables during the experience. In a purely Lagrangian study, the point of view is linked to each particle and we study around this particle physical variables as a function of time. In an ALE approach, the point of view is linked to a mesh, which is embedded in the fluid. We choose its physical speed $\vec{W}$. It is not necessary equal to $\vec{0}$ (as in Eulerian formulation) or to the fluid velocity $\vec{V}$ (as in Lagrangian formulation). It can vary arbitrarily and smoothly from $\vec{0}$ to $\vec{V}$. Thus, the ALE formulation will be purely Lagrangian or purely Eulerian where it is needed, and hybrid everywhere else.

In the following, we present in details the ALE formulation and the general algorithm which is usually used (see also [7]). We close this overview with a discussion on the advantages and drawbacks of the method.

Formulation :

• In the following, we will consider spatial coordinates and derivatives in the physical space of the laboratory. This spatial coordinates will be denoted $\vec{x}$. We will also work with Lagrangian variables $\vec{a}$. Holding the vector $\vec{a}$ fixed means following the corresponding particle in its motion.

• A physical variable "g" will be tilded $\tilde{g}$ when it is considered as a function of the Lagrangian variables $(\vec{a}, t)$. The notation g will be used only if the variable is considered as a function of the Eulerian coordinates $(\vec{x}, t)$.

• The ALE formulation uses mixed coordinates. They depend on Lagrangian coordinates $(\vec{a}, t)$ and will be denoted

$$\overrightarrow{\xi} = \overrightarrow{\xi}(\vec{a}, t) \tag{25}$$

For simplicity, we will write $\vec{\xi}$ instead of $\tilde{\vec{\xi}}$. We will write subscripted variables when they are held constant in evaluating partial derivatives. We define the mixed Jacobian and the mesh speed by :

$$\tilde{J}(\vec{a}, t) = \det\left[\left.\frac{\partial \vec{\xi}}{\partial \vec{a}}\right|_t (\vec{a}, t)\right] \tag{26}$$

$$\widetilde{\vec{W}}(\vec{a}, t) = \left.\frac{\partial \vec{\xi}}{\partial t}\right|_{\vec{a}} (\vec{a}, t). \tag{27}$$

This Arbitrary Lagrangian-Eulerian description is summerized on figure 4.

• For this formulation, we will also need a pass from Lagrangian coordinates to Eulerian coordinates. For any function $\tilde{g}$ of Lagrangian coordinates, we define the function $\bar{g}$ of spatial coordinates by :

$$\bar{g}(\vec{x}, t) = \tilde{g}(\vec{a}, t) \text{ where } \vec{a} \text{ is such that } \vec{x} = \vec{\xi}(\vec{a}, t). \tag{28}$$

At the same time, we also need a pass from Eulerian coordinates to Lagrangian coordinates. For any function $\bar{g}$ of spatial coordinates we define the function $\tilde{g}$ of Lagrangian coordinates by :

$$\tilde{g}(\vec{a}, t) = \bar{g}(\vec{x}, t) \text{ where } \vec{x} \text{ is given by : } \vec{x} = \vec{\xi}(\vec{a}, t). \tag{29}$$

In both correspondences, we then have the identity

$$\bar{g}(\vec{\xi}(\vec{a}, t), t) = \tilde{g}(\vec{a}, t). \tag{30}$$

• We will use two general lemmas, which can be proved in the same way as Lemmas 3 and 4

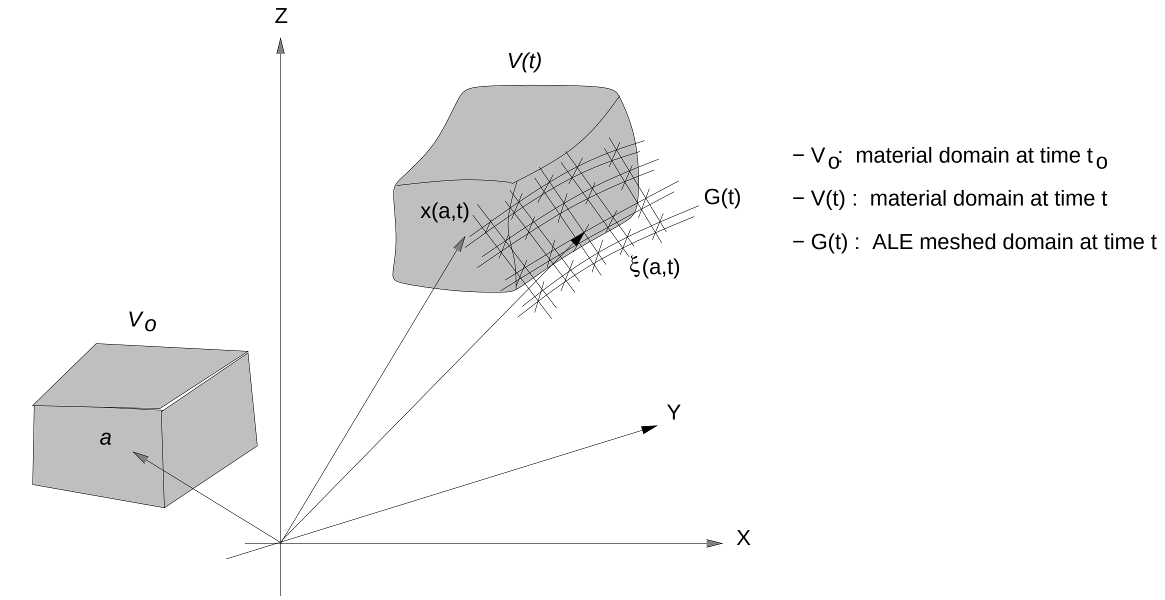
Z
V(t)
x(a,t)
G(t)
ξ(a,t)
V0
a
Y
X
− V0: material domain at time t0
− V(t) : material domain at time t
− G(t) : ALE meshed domain at time t

Figure 4: Lagrangian, Eulerian and mixed variables in the ALE description.

below. Both lemmas are purely algebraic. They include no physical considerations. The first one gives a differential equation for the mixed Jacobian $\widetilde{J}$ defined above.

Lemma 1 *$\widetilde{J}$ is solution of the following partial differential equation :*

$$\left.\frac{\partial \widetilde{J}}{\partial t}\right|_{\vec{a}} (\vec{a},t) = \widetilde{J}(\vec{a},t)\, div_{\vec{\xi}}(\bar{\vec{W}}) \left(\vec{\xi}(\vec{a},t),t\right). \tag{31}$$

The second lemma gives a mean to have a translation from Lagrangian-type time-derivatives with the material coordinates held constant to Eulerian-type time-derivatives with spatial coordinates held constant.

Lemma 2 *For any scalar quantity g, we have :*

$$\left.\frac{\partial (\widetilde{J}\tilde{g})}{\partial t}\right|_{\vec{a}} (\vec{a},t) = \widetilde{J}(\vec{a},t) \left[\left.\frac{\partial \bar{g}}{\partial t}\right|_{\vec{\xi}} + div_{\vec{\xi}}(\bar{g}\bar{\vec{W}}) \right] \left(\vec{\xi}(\vec{a},t),t\right) \quad . \tag{32}$$

• Let us consider the vector of conservative variables $\bar{Q}$ (3), function of Eulerian coordinates and the corresponding Lagrangian function $\tilde{Q}$ defined by (29). We can apply the preceding lemma to each scalar component of $\tilde{Q}$. Since $\bar{Q}$ is solution of Euler equations, we obtain the following general ALE formulation :

$$\boxed{\left.\frac{\partial (\widetilde{J}\tilde{Q})}{\partial t}\right|_{\vec{a}} (\vec{a},t) + \widetilde{J}(\vec{a},t)\, div_{\vec{x}} \left[(\bar{E},\bar{F}) - \bar{Q} \otimes \bar{\vec{W}}\right] \left(\vec{\xi}(\vec{a},t),t\right) = 0.} \tag{33}$$

which can be expanded in :

$$\left\{\begin{array}{llll} \left.\dfrac{\partial(\widetilde{J}\widetilde{\rho})}{\partial t}\right|_{\vec{a}}(\vec{a},t) & +\widetilde{J}(\vec{a},t)\,\left[div_{\vec{x}}\left[\overline{\rho(\vec{V}-\vec{W})}\right]\right]\left(\vec{\xi}(\vec{a},t),t\right) & & =0, \\ \left.\dfrac{\partial(\widetilde{J}\widetilde{\rho u})}{\partial t}\right|_{\vec{a}}(\vec{a},t) & +\widetilde{J}(\vec{a},t)\,\left[div_{\vec{x}}\left[\overline{\rho u(\vec{V}-\vec{W})}\right]+\bar{P}_x\right]\left(\vec{\xi}(\vec{a},t),t\right) & & =0, \\ \left.\dfrac{\partial(\widetilde{J}\widetilde{\rho v})}{\partial t}\right|_{\vec{a}}(\vec{a},t) & +\widetilde{J}(\vec{a},t)\,\left[div_{\vec{x}}\left[\overline{\rho v(\vec{V}-\vec{W})}\right]+\bar{P}_y\right]\left(\vec{\xi}(\vec{a},t),t\right) & & =0, \\ \left.\dfrac{\partial(\widetilde{J}\widetilde{e})}{\partial t}\right|_{\vec{a}}(\vec{a},t) & +\widetilde{J}(\vec{a},t)\,\left[div_{\vec{x}}\left[\overline{e(\vec{V}-\vec{W})+P\vec{V}}\right]\right]\left(\vec{\xi}(\vec{a},t),t\right) & & =0. \end{array}\right. \tag{34}$$

It may be easily verified that these equations take the form of Lagrangian equations when we have uniformly $\vec{W}=\vec{V}$, and they reduce to classical Euler equations when $\vec{W}=\vec{0}$.

• We can now obtain an interesting formulation. We integrate equation (33) on an elementary volume of the material space. Time derivatives with the material coordinates held constant can be put out of the integral signs. Using a change of coordinates from $\vec{a}$ to $\vec{\xi}$, we can write :

$$\boxed{\frac{\partial}{\partial t}\int_{V_{\vec{\xi}}(t)}\bar{Q}d\vec{\xi}+\int_{V_{\vec{\xi}}(t)}div_{\vec{x}}\left(F(\bar{Q})-\bar{Q}\otimes\bar{W}\right)d\vec{\xi}=0.} \tag{35}$$

We will see that this formulation, where all materials coordinates have disappeared, is also used (in a different way) in dynamic meshes methods.

Algorithm :

The general algorithm for ALE methods is different from all other algorithms used in fluid-structure interaction. Though the formulation is very similar to dynamic meshes methods, the time-integration is based on a two step algorithm which excludes global upwind schemes. On the other hand, the goal of this specific formulation is the elegant and simultaneous integration of actions of the fluid and the structure on one another.

• In the first step, we calculate the Lagrangian nodal velocities resulting from the pressure and body forces of the previous time step. Supposing that $\vec{W}=\vec{V}$, we compute the Lagrangian part of the second integral in (35). This phase and the computation of the motion of the structure can be performed at the same time. They can be integrated in time with implicit schemes. At the end of this step, we know the location, speed and acceleration of the structure after the time step and we have computed the Lagrangian part of the flow's evolution.

• The second step executes two tasks. Knowing all characteristics of the structure's motion, we can affect new values to $\vec{W}$ and update the mesh. We also have to compute the convective part of the fluxes, due to the new mesh speed $\vec{W}$. The first task can be completed with one of the mesh updating schemes we already presented in (12) and (13). The second one is not very complex. It includes among others the computation of the new cell volumes. Mass, momentum and energy convective fluxes are added to Lagrangian fluxes to complete the integration.

Advantages and Drawbacks :

It is clear that Arbitrary Lagrangian-Eulerian methods have several advantages. First, they use very simple equations. They are just a little more complex than the original fluid dynamics equations, because of Jacobians and mixed coordinates speeds. Second, this kind of method can deal with all types of geometries since the mesh can be of any form (and in particular unstructured). Third, the Lagrangian step of the integration allows a real interaction simulation. During this step, since all cells are considered closed (no convection through interfaces), the fluid and the structure play similar roles. In some sense, we have taken into account that the action of the structure on the fluid and the action of the fluid on the structure are opposite.

However, this formulation has also drawbacks. Though it is valid for all configurations, it is not necessarily optimal. The formulation could be slightly changed in particular cases, rigid-body motions for example. Moreover, the splitting in Lagrangian and convective fluxes can give time accurate solutions only for very small time steps. The problem of good interaction resolution has been transferred to this Lagrangian-convective fluxes splitting. Last drawback but not least, these methods do not match with global upwind schemes, which allow good computational efficiency and robustness.

In short, the Arbitrary Lagrangian-Eulerian formulation produces original methods different from fixed computer domain methods with moving frames of reference. The formulation is general and treats the fluid-structure interaction in an elegant way. However, the splitting between Lagrangian and convective fluxes reduces the global accuracy for large time steps. We will now see the family of methods using so-called dynamic meshes. Their formulation is very near from an ALE formulation, but it is much more precise. Treatments of boundaries are classical and global upwind schemes can be used.

2.4 Methods using dynamic meshes.

These methods are formulated on dynamic meshes, which means that the cells of the spatial discretization have their own absolute speed – possibly different from zero and from the fluid speed. This kind of formulation do not explicitly use the forms of the cells (triangle, quadrangle...) and the type of the grid (structured or unstructured). The methods can therefore used on unstructured meshes, which is an important advantage in comparison with fixed computational domain methods. The formulation in dynamic meshes is slightly different from Arbitrary Lagrangian-Eulerian formulation since no reference to Lagrangian coordinates is made.

Formulation :

- The first way to obtain the final formulation looks like an ALE approach. Let $\vec{\xi}$ be a mixed geometric variable. The iso-ξ_i curves can be the mesh lines if the grid is structured. Both variables $\vec{x}$ and $\vec{\xi}$ are time dependent functions of each other, as

$$\vec{\xi} = \vec{\xi}(\vec{x}, t) \qquad \text{and} \qquad \vec{x} = \vec{x}(\vec{\xi}, t). \tag{36}$$

Differentiating from the last equation, let J and $\vec{w}$ be the following quantities :

$$J = \det \left(\left. \frac{\partial \vec{x}}{\partial \vec{\xi}} \right|_t \right) \tag{37}$$

and

$$\vec{w} = \left. \frac{\partial \vec{x}}{\partial t} \right|_{\vec{\xi}} \quad . \tag{38}$$

The subscripted variables are held constant in partial derivatives and the following notations are used hereunder :

$$\overrightarrow{\nabla}_{\vec{x}} g = (\frac{\partial g}{\partial x_1}, \ldots, \frac{\partial g}{\partial x_D})^t \qquad \text{and} \qquad div_{\vec{x}}(\vec{g}) = \sum_i \frac{\partial g_i}{\partial x_i}.$$

Lemma 3 *We have the following partial differential equation for J :*

$$\left. \frac{\partial J}{\partial t} \right|_{\vec{\xi}} = J \; div_{\vec{x}}(\vec{w}) \tag{39}$$

Proof :
We have (writing Tr for the trace operator)

$$div_{\vec{x}}(\vec{w}) = \sum_i \frac{\partial w_i}{\partial x_i} = \sum_i \sum_j \frac{\partial w_i}{\partial \xi_j} \frac{\partial \xi_j}{\partial x_i} = Tr(\left[\frac{\partial \vec{w}}{\partial \vec{\xi}} \right] \left[\frac{\partial \vec{\xi}}{\partial \vec{x}} \right]). \tag{40}$$

If we write $\mathcal{J}$ for $\partial \vec{x} / \partial \vec{\xi}$, noticing that $\partial \vec{w} / \partial \vec{\xi} = \partial \mathcal{J} / \partial t \overset{\text{def}}{=} \mathcal{J}'$, we deduce from (40)

$$div_{\vec{x}}(\vec{w}) = Tr(\mathcal{J}' \mathcal{J}^{-1}). \tag{41}$$

For s small enough, we have

$$\mathcal{J}(t+s) = \mathcal{J}(t) \left(Id + s \mathcal{J}(t)^{-1} \mathcal{J}'(t) + o(s) \right) = \mathcal{J} \exp(s \mathcal{J}^{-1} \mathcal{J}') + o(s). \tag{42}$$

Since the determinant is a continuous function, using identities such as $Tr(AB) = Tr(BA)$ and $det(\exp(sA)) = \exp(s \; Tr(A))$, we obtain

$$J(t+s) = J(t) \exp(s \; Tr(\mathcal{J}' \mathcal{J}^{-1})) + o(s) = J(t) + s \; J(t) Tr(\mathcal{J}' \mathcal{J}^{-1}) + o(s), \tag{43}$$

and then

$$J' = J \; Tr(\mathcal{J}' \mathcal{J}^{-1}). \tag{44}$$

Equations (41) and (44) give the proof $\diamondsuit$

From the preceding lemma, we deduce

Lemma 4 *For any scalar quantity g, we have :*

$$\left.\frac{\partial(Jg)}{\partial t}\right|_{\vec{\xi}} = J \ \left(\left.\frac{\partial g}{\partial t}\right|_{\vec{x}} + div_{\vec{x}}(g\vec{w})\right) \quad . \tag{45}$$

Proof :
The classical chain relation from $\vec{\xi}$-derivatives to $\vec{x}$-derivatives takes the form

$$\left.\frac{\partial g}{\partial t}\right|_{\vec{\xi}} = \left.\frac{\partial g}{\partial t}\right|_{\vec{x}} + \overrightarrow{\nabla}_{\vec{x}} g . \left.\frac{\partial \vec{x}}{\partial t}\right|_{\vec{\xi}} . \tag{46}$$

Multiplying by J and using the definition of $\vec{w}$, we obtain

$$J \ \left.\frac{\partial g}{\partial t}\right|_{\vec{\xi}} = J \ \left.\frac{\partial g}{\partial t}\right|_{\vec{x}} + J \ \overrightarrow{\nabla}_{\vec{x}} g . \vec{w} \quad . \tag{47}$$

If we multiply both sides of (39) by g and add it to (47), we obtain (45) since

$$div_{\vec{x}}(g\vec{w}) = g \ div_{\vec{x}}(\vec{w}) + \overrightarrow{\nabla}_{\vec{x}} g . \vec{w} \ \ \diamondsuit$$

If we apply Lemma 4 to the conservative variables ρ, ρu, ρv and e, we have the following equation :

$$\boxed{\left.\frac{\partial(JQ)}{\partial t}\right|_{\vec{\xi}} + J \ div_{\vec{x}} \vec{\bar{F}} = 0} \tag{48}$$

where

$$\bar{F}_x = \begin{pmatrix} \rho\bar{u} \\ \rho u\bar{u} + p \\ \rho v\bar{u} \\ e\bar{u} + pu \end{pmatrix}, \quad \bar{F}_y = \begin{pmatrix} \rho\bar{v} \\ \rho u\bar{v} \\ \rho v\bar{v} + p \\ e\bar{v} + pv \end{pmatrix} \quad \text{and} \quad \left| \begin{array}{l} \bar{u} = u - w_x \\ \bar{v} = v - w_y \end{array} \right. \quad . \tag{49}$$

It is here interesting to notice that the meaning of these equations is fully conserved for special cases of our variable coordinate $\vec{\xi}$. The case where $\vec{\xi}(\vec{x},t) = \vec{x}$ gives for (48) and (49) the classical Euler equations (since $\vec{w} = \vec{0}$). The case where $\vec{\xi}(\vec{x},t) = \vec{a}(\vec{x},t)$ is the Lagrangian material coordinate of the particle located in $\vec{x}$ at time t gives the usual Lagrangian equations of gas dynamics.

• We can obtain an integral formulation of (48) identical with the formulation used by Batina in [2]. Let us call C a cell of our discretization. This cell occupies respectively the domains $C_{\vec{x}}$ in $\vec{x}$-coordinates and $C_{\vec{\xi}}$ in $\vec{\xi}$-coordinates. We suppose that $C_{\vec{\xi}}$ is not time-dependent. Integrating (48) over $C_{\vec{\xi}}$, we find

$$\int_{C_{\vec{\xi}}} \left.\frac{\partial(JQ)}{\partial t}\right|_{\vec{\xi}} d\vec{\xi} + \int_{C_{\vec{\xi}}} J \ div_{\vec{x}} \vec{\bar{F}} \, d\vec{\xi} = 0.$$

Since the time-derivative is done with $\vec{\xi}$ held constant and since $C_{\vec{\xi}}$ does not vary in time, we can put it out of the integral. Then, using the change of variables $\vec{\xi} = \vec{\xi}(\vec{x}, t)$ and $d\vec{x} = J\, d\vec{\xi}$, we finally get

$$\boxed{\frac{d}{dt}\left[\int_{C_{\vec{x}}} Q\, d\vec{x}\right] + \int_{C_{\vec{x}}} div_{\vec{x}}\vec{\vec{F}}\, d\vec{x} = 0.} \tag{50}$$

We remind that this formula is valid when $C_{\vec{x}}$ is a spatial domain corresponding to a fixed domain $C_{\vec{\xi}}$ of mixed coordinates. This last integration formula can be used for a finite-volume formulation. Using averages on cells, we will write

$$A_i^{n+1}Q_i^{n+1} - A_i^n Q_i^n + \Delta t \sum_{j=1}^{n(i)} \|\widetilde{\partial C_{ij}}\|.\bar{\Phi}(Q_i, Q_j, \widetilde{\vec{\eta_{ij}}}) = 0, \tag{51}$$

where Q_i^n is the average of Q on cell C_i at time t_n, A_i^n is the area of cell C_i at time t_n, Δt is the time step, $n(i)$ is the number of neighbour cells for C_i, $\widetilde{\partial C_{ij}}$ is a time-mean interface between the cell C_i and its neighbour C_j (of length $\|\widetilde{\partial C_{ij}}\|$ and normal $\widetilde{\vec{\eta_{ij}}}$ oriented from C_i to C_j) , and $\bar{\Phi}$ is a numerical flux such that

$$\Delta t\, \|\widetilde{\partial C_{ij}}\|.\bar{\Phi}(Q_i, Q_j, \widetilde{\vec{\eta_{ij}}}) \simeq \int_{t^n}^{t^n+\Delta t} \left[\int_{\partial C_{ij}} \vec{\vec{F}}.\vec{\eta_{ij}}\, d\sigma\right] d\tau \tag{52}$$

The reader will find in [12] a general one-dimensional formulation for Godunov-type schemes on moving meshes. For the resolution of (48), we can make use of global upwind differencing and flux-vector splitting schemes similar to those developed for computations on structured meshes. For example, it may be deduced from (52) an expression for Roe's method on moving grids in a very classical way [12]. In a two-dimensional case, the expression for Roe's numerical flux would take the form :

$$\bar{\Phi}(Q_i, Q_j, \vec{\eta}) = \frac{1}{2}\left[\left(\vec{\vec{F}}_i + \vec{\vec{F}}_j\right).\vec{\eta} - \left|\tilde{A} - (\vec{w}.\vec{\eta})I\right|(Q_i - Q_j)\right], \tag{53}$$

where $\tilde{A}$ is Roe's matrix for the flux $E\eta_x + F\eta_y$ and the sign $|\ |$ is taken on the matrix after diagonalization.

We now have to make two remarks on the preceding equation. First, it may be easily shown that the numerical flux $\bar{\Phi}$ depends only on $\vec{w}$ through its normal component $\vec{w}.\vec{\eta}$. Second, since the grid is moving, the field of grid speed $\vec{w}$ varies with time. We should have used average values $\vec{w}$, $\widetilde{\partial C_{ij}}$ and $\tilde{\vec{w}}.\widetilde{\vec{\eta_{ij}}}$ in (49) and (53). We still have to make a choice for the preceding averaged tilded quantities.

The same expressions as (53) can be obtained with a spatio-temporal approach of the problem. In [23], N'Konga and Guillard consider spatio-temporal work-volumes generated by the deforming cells C_i during a time step. Integrating unsteady Euler equations on these volumes, they finally get the same formulation (51). Furthermore, they give a justification for a natural choice for $\widetilde{\partial C_{ij}}$ and $\tilde{\vec{w}}.\widetilde{\vec{\eta_{ij}}}$. We will see below the main principle of this justification. Calling P_{ij1} and P_{ij2} the ends of ∂C_{ij}, they decide that $\widetilde{\partial C_{ij}}$ is the segment whose ends are the mean position of P_{ij1} and P_{ij2} during the time step and that

$$\tilde{\vec{w}}.\widetilde{\vec{\eta_{ij}}} = \frac{1}{2}\left(\vec{w}(P_{ij1}) + \vec{w}(p_{ij2})\right).\widetilde{\vec{\eta_{ij}}}. \tag{54}$$

This extension for moving meshes has already been done for many different methods : for instance, Roe's approximate Riemann solver with several orders of accuracy [15] or Van Leer's flux-vector splitting [3].

Algorithm :

• The first phase of each time step is the integration of (48) with the method given by (51), (52) and (53).

• In a second phase, we must update all geometric variable needed in the first phase. The updating scheme for $\vec{w}$ may follow (12) or (13) like for fixed computational domain methods. This very simple algorithm can get along with all inventions for unstructured meshes, like adaptive refinement [19](also consistent with ALE formulations) or multigrid methods [21].

Since we use for each cell the areas in (51), we have to update them abiding by the geometric conservation law [29]. As for (14), we have to update the cells areas with the same scheme as for a uniform field Q. Then the scheme should be :

$$A_i^{n+1} - A_i^n + \Delta t \sum_{j=1}^{n(i)} \|\widetilde{\partial C_{ij}}\|.(-\tilde{\vec{w}}.\widetilde{\vec{\eta_{ij}}}) = 0. \tag{55}$$

We then have to choose $\widetilde{\partial C_{ij}}$ and $\tilde{\vec{w}}.\widetilde{\vec{\eta_{ij}}}$ such that the area $\mathcal{S}$ covered by ∂C_{ij} during a time step Δt verifies

$$\mathcal{S} \simeq \Delta t \, \|\widetilde{\partial C_{ij}}\| \left(\tilde{\vec{w}}.\widetilde{\vec{\eta_{ij}}}\right). \tag{56}$$

The formulas given by N'Konga and Guillard in [23] are built in order to have the best approximation of S with $\widetilde{\partial C_{ij}}$ and $\tilde{\vec{w}}.\widetilde{\vec{\eta_{ij}}}$ in (56).

Since this updating scheme corresponds to (51) for a scalar variable constant and equal to one, the geometric conservation law will not be transgressed [29]. The scheme is simple and will not generate unstabilities. It is exactly the same scheme as presented in the first section for body-fitted curvilinear coordinates.

Advantages and Drawbacks :

This method gathers lots of advantages. First, global upwing schemes can be used, which was not the case for the ALE formulation. Second, no geometric elements but the cells areas are used. They have to be updated after each time step, but the scheme (55) is simple, conservative and avoids the numerical unstabilities shown in [29]. The only drawback of the method is the need of an grid updating phase after each time-step. Though dynamic meshes method may be less efficient than the one presented by Lin in [18], it is certainly more general. Furthermore, according to Batina [2], the mesh updating scheme with prediction-correction based on strings gives efficient results.

2.5 Conclusion.

In this section, we surveyed several methods for the resolution of gas dynamics in moving boundaries problems. The model equations have been the Euler equations (2–3). Start point for all explanations, they have been written differently : we have seen Euler equations in body-fitted curvilinear coordinates (5–6), their new form in body-fitted coordinates and moving frames of reference (21) and finally their integral form in the ALE formulation and dynamic meshes methods (35–50).

We can notice that the latter formulas (35–50) are very close to each other. In both formulas, all material coordinates have disappeared. On the contrary, we still have derivatives with the spatial coordinates held constant. At this point, we can make two remarks. First, the whole ALE formulation was certainly not optimal. It should have been derived with only two systems of coordinates : the mixed coordinates $\vec{\xi}$ and either the Lagrangian coordinates or the Eulerian coordinates. Obviously, this other system of coordinates should be the Eulerian coordinates for very general cases. It could be pseudo-Lagrangian coordinates for special cases (for example, the case of a two-dimensional rigid wing profile in an external flow : the coordinates should be linked to the profile). Second, ALE methods and dynamic meshes methods only differ in the use they make of the integral formulation. In pure ALE methods, a Lagrangian phase and a convective phase are performed during each time step. Pure ALE methods are mostly used in hydroelastic studies [7].

All methods presented above are quite general. They just consist in looking at the model equations from different points of view. Thus, they can be applied to potential formulations (three-dimensional transonic small disturbances for unsteady inviscid flow [4] and three-dimensional unsteady full potential equation [28]) or Navier-Stokes equations (unsteady three-dimensional body-fitted version [11]).

For all presented methods, we have not written in detail the boundary conditions. These boundary conditions actually produce no additional difficulties. In each specific formulation, they are to be translated in the frames or coordinates under consideration. Their underlying physical principles do not change. For example, on the far-field fluid boundary, the flow is fixed in a galilean frame of reference; this condition is possibly tranlated and introduced directly or with the method of characteritics. On the surface of the moving/deforming structure, the translation of the slip condition is enforced or induced by wall fluxes.

Heretofore, the motion and the deformation of the structure and the flow boundaries have been supposed known. We used them for the expression of the fluid boundary conditions and for all general geometric updating schemes. We can consider that we just dealt with the action of the structure on the fluid. In the next section, we will handle the question of the interaction. We will study how to include the dependence of the structure's motion on the flow.

3 Fluid-structure interaction.

In this section, we want to deal more precisely with the interaction at the interface between the fluid and the structure. This kind of interaction has the same characteristics in aeroelasticity, hydroelasticity or any fluid structure coupling phenomenon. In the following, we first study this interaction and the possible ways to perform a numerical simulation. Then, we present the most simple, general and used algorithm for interaction computations.

3.1 The cycle of interaction.

The coupling phenomenon between the fluid and the structure, this so-called interaction, can be understood with the idea of a cycle, covered instantaneously and constantly by an imaginary operator responsible for physical phenomena. During the evolution of the fluid and the structure, the movement and/or deformation of the shape of the structure induces at once a change in the flow. This induction is made through the location and the own speed of the boundary for the external flow. Since the flow changes, the pressure field on the structure varies and the movement and/or deformation of the shape changes. And again this last change induces a variation in the flow... We see that the variation of the flow and the movement of the structure are coupled phenomena. They affect each other through boundary conditions from structure to fluid and through pressure field (or viscous efforts) from fluid to structure.

Nearly all the methods used in aeroelasticity are based on this simple cycle. Such methods use a staggered solution strategy. There exist also pressure elimination strategies and simultaneous solution which are computationnaly prohibitive [25]. ALE methods also are exceptions to this general agreement in some sense. We will explain later why. Other methods could be summed up as follows :

$$S^n \xrightarrow{1} B^n \overset{2}{\Longrightarrow} F^n \xrightarrow{3} P^n \overset{4}{\Longrightarrow} S^{n+1} \xrightarrow{5} B^{n+1} \overset{6}{\Longrightarrow} F^{n+1} \cdots$$

In the preceding scheme, the superscripts correspond to the time level. Respectively, S, B, F and P represent the state of the structure, the boundary conditions for the fluid problem, the state of the fluid and the pressure field on the structure's surface. The double arrows $\Longrightarrow$ represent heavy computations : for example, the state of the fluid after an elementary time step knowing the boundary conditions ($\overset{2}{\Longrightarrow}$), or the state of the structure after a time step knowing the pressure ($\overset{4}{\Longrightarrow}$). The simple arrows $\longrightarrow$ represent obvious computations like getting the boundary conditions for the flow knowing the state of the structure ($\xrightarrow{1}$) or the pressure field knowing the state of the fluid ($\xrightarrow{3}$).

The scheme for the interaction cycle can be applied to various physical problems [28]. For static rigid computations (only steady aerodynamics), phase 2 is only performed. The pseudo-unsteady scheme should converge towards the steady solution. For dynamic rigid computations, all phases are performed, but phase 4 is rather light since the structure has few degrees of freedom. For flexible cases, all phases are totally performed. Static flexible cases can be quite interesting. For example, an elastic panel in the wind (see figure 5 for static cases). Flutter problems on airplanes are all dynamic cases.

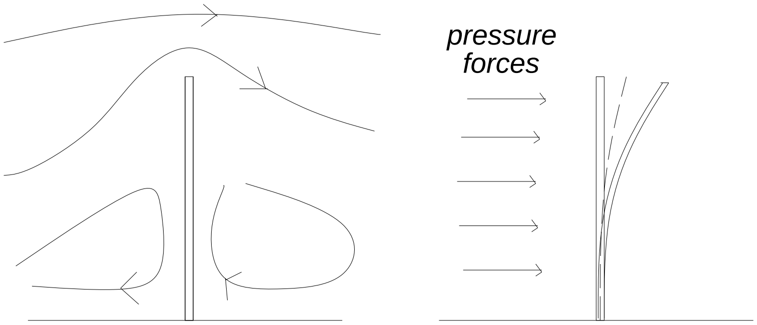

Figure 5: static rigid and static flexible cases.

The superscripts in the scheme hide an interesting difficulty. During phase 2, the speed of the movind and/or deforming shape is held constant. During phase 4, the flow is supposed constant. Thus, comparing with the structure, the flow is a little late. It is obvious that we could have started writing superscripts $n+1$ in the scheme after another phase of the cycle. In that case, the structure would have been a little late. This little problem is in general overcome by taking time steps small enough. Since the typical time of evolution is much smaller for the fluid than for the structure, aeroelasticians have rather the structure late. The following choice is then mostly made :

$$S^n \xrightarrow{1} B^n \xRightarrow{2} F^{n+1} \xrightarrow{3} P^{n+1} \xRightarrow{4} S^{n+1} \xrightarrow{5} B^{n+1} \xRightarrow{6} F^{n+2} \cdots \qquad (57)$$

It may be a little surprising that we dispose only of two staggered schemes, the last one being the best (57). In reality, the coupling between the structure and the fluid is present constantly, and, the actions of the fluid on the structure and of the structure on the fluid are simultaneous and opposite. Only ALE methods take into account the simultaneity of both actions. It is done in the first (Lagrangian) phase of each integration step. But the quality of the ALE algorithm also depends on the validity of the Lagrangian-convective splitting of fluxes for large time steps.

Because of the constant coupling of both elements, the simulation may be more accurate if we have simultaneous integrations for the fluid and the structure. But this kind of simulation would require among others estimates of complex abstract functions giving dependances on the structure's shape of its action on the outer domain or the action of the fluid on it, through the pressure field. The first function could be given by structural dynamists if the mechanics were linear. Different versions of the second one exist for several structural dynamics problems.

Dynamists use these approximate formulas when they want to limit their study to their speciality. For example, Lottati [20], in a study on the role of structural and aerodynamic damping on the aeroelastic behavior of wings, used such approximate formulas for the dependance of unsteady aerodynamic forces and moments on the reduced frequency of an oscillating wing. In [16], Lin et al. worked on plates flutter and used a linearized potential model (stemming from the unsteady lifting surface theory coupled with the doublet-lattice method [5]) for subsonic fluid flows. They obtained formulas such as the integral equation

$$\frac{v(\vec{x})}{u_\infty} = \frac{1}{8\pi}\int_{surf} \Delta C_p(\vec{x_s}).K(\vec{x}-\vec{x_s})d\vec{x_s}, \tag{58}$$

which gives the expression of the vertical fluid's speed around a wing as a function of the pressure field (K is a kernel function representing the downwash at $\vec{x}$ induced by a unit impulse load at $\vec{x_s}$). Sarma and Varadan studied in [26] a nonlinear panel flutter under supersonic flow with the help of quasisteady supersonic flow theory, and used expression converse of (58) such as the following expression (where M_∞ is the freestream Mach number) :

$$\Delta C_p = \left(\frac{-2}{\sqrt{M_\infty^2-1}}\right)\left[\frac{\partial v}{\partial x} + \frac{1}{u_\infty}\left(\frac{M_\infty^2-2}{M_\infty^2-1}\right)\frac{\partial v}{\partial t}\right]. \tag{59}$$

These methods avoid aerodynamic computations. They use good approximations of phenomema which take place in the flow, but they are only valid for very specific cases (totally subsonic or supersonic) and they use linearizations. Thus, they may give very poor results for complex studies like transonic flows or very nonlinear phenomena.

In short, we have seen that all methods use the same time step for the fluid and the structure, which is certainly necessary to get time-accurate simulations. However, the actual simultaneous integration of the structure and the fluid is not practised. All methods are based on staggering schemes, which – up to now – seem to enforce very strong limitations of the time step. These limitations have been theoretically explained in some interesting cases [25]. The simultaneous integration of both actions may probably be a necessary step towards implicit integration of fluid-structure interaction simulations.

3.2 General algorithm.

We describe now the process summed up on the scheme (57). We use the same notations and we write $\dot{S}$ and $\ddot{S}$ for the speed and acceleration of the structure. In Table 1, the downwards vertical axis represents the CPU-time during the computation. We suppose that we have saved at the beginning of a time step the state of the fluid F, the state of the structure (and its speed and acceleration) S, $\dot{S}$ and $\ddot{S}$. We also know all geometric variables (mesh, Jacobians, etc...) and the geometric speeds (grid speeds and possibly variables corresponding to moving frames of reference).

Since we use the idea of a cycle of interaction, Table 1 is cyclic. In fact, only six lines are performed during each time step of the integration. The second line is only performed for FCD methods with moving frames of reference. Heavy aerodynamic computations are performed in line 4 and heavy structural dynamics computations are done in line 6.

We have already discussed how to perform some lines of the general algorithm. The mesh for a new time step is computed with formulas (12) or (13). The metrics are then deduced according to (11) if curvilinear coordinates are used. Moving frames of reference are possibly

VARIABLES COMPUTED	VARIABLES USED
mesh and metrics at t^n	$S(t^n)$
moving frames of reference at t^n	$S(t^n)$ and $\dot{S}(t^n)$
boundary conditions $B(t^n)$	$S(t^n)$ and $\dot{S}(t^n)$
state of the fluid $F(t^{n+1})$	$F(t^n)$, $B(t^n)$, whole geometry
surface pressure field $P(t^{n+1})$	$F(t^{n+1})$
$S(t^{n+1})$, $\dot{S}(t^{n+1})$ and $\ddot{S}(t^{n+1})$	$P(t^{n+1})$, $S(t^n)$, $\dot{S}(t^n)$ and $\ddot{S}(t^n)$
mesh and metrics at t^{n+1}	$S(t^{n+1})$
moving frames of reference at t^{n+1}	$S(t^{n+1})$ and $\dot{S}(t^{n+1})$
boundary conditions $B(t^{n+1})$	$S(t^{n+1})$ and $\dot{S}(t^{n+1})$
state of the fluid $F(t^{n+2})$ $\vdots$	$F(t^{n+1})$, $B(t^{n+1})$, whole geometry $\vdots$

Table 1: The general form of staggering algorithms.

updated with respect to the movement of the structural element they are linked to. Boundaries are given new locations and new walls normal speeds are computed. The state of the fluid at the next time step is the result of an aerodynamic integration. This integration is not based on the classical Euler equations (2), but on equations modified by use of curvilinear body-fitted coordinates (5) or multiple moving frames of reference (16) or both of them (21). It can also be based on a dynamic mesh formulation (48), with an integral form (50).

In short, we have described very precisely the global staggering algorithm used for fluid-structure interaction simulations. In the first section, we had presented numerical methods for moving boundaries problems. In such problems, the motions of the boundaries are predetermined. They are used to update after each time-step the mesh, the metrics and their time-derivatives, and/or the moving frames of reference. Since they are preset, these motions do not depend on the flow. But, in fluid-structure interaction simulations, the motions of the structure are not predetermined. We will see, in the next section, the structural part of aeroelastic simulations. We will show models for the motions of the structure and numerical schemes for the time integration of these motions.

4 Structural dynamics.

In this section, we study the methods commonly used by aeroelasticians to compute the structural dynamics part of their numerical simulations.

In fluid-structure interaction simulations, the structure evolves dynamically under external forces (pressure on the surface, gravity). We suppose that the mechanical response of the structure is linear and elastic. Since we use the general algorithm presented in Table 1, we will have to compute the location, speed and acceleration of the structure at a new time step t^{n+1} using their values at time t^n and the action of the fluid at time t^{n+1} (the structure is therefore a little late).

In the following, we present the model equations for the structure and the method of discretization fot its motion. Then, we propose numerical schemes for the time integration from t^n to t^{n+1}.

4.1 Structural model equations.

Since the structure considered is continuous, the set of its displacements is a space of infinite dimension. We use a finite-element type of discretization to reduce the space of displacements to a finite dimension (which is number of degrees of freedom in the discretization). In a second step, using Lagrange's equation, we write a general model equation for the aeroelastic motion of the structure. We can also compute structural modes from this equation and obtain a modal equation for the motion.

Discretization.

• We use a finite-element type discretization (see e.g. [5]). It is assumed that the elastic deformation of the continuous structure can be represented by deflections at a set of discrete control points. Thus, the displacement r is taken of the form

$$r = \sum_{i=1}^{n} \left(\frac{\partial r}{\partial q_i} \right) . q_i, \tag{60}$$

where n is the finite dimension of the discretization space, $\partial r / \partial q_i$ are basis functions and q_i are called generalized coordinates.

• Using the definition (60) and writing doted signs for time derivatives, we can give the expressions for kinetic, elastic and dissipated energies.

∘ The kinetic energy T is given by :

$$T = \frac{1}{2} \int \rho \, \dot{r}^t . \dot{r} = \frac{1}{2} \dot{q}^t M \dot{q}, \tag{61}$$

where ρ is the density of the structure and M is the $(n \times n)$ generalized mass matrix. Its term on k^{th} line and l^{th} column is given by :

$$M_{k,l} = \int \rho \left(\frac{\partial r}{\partial q_k}\right)^t \left(\frac{\partial r}{\partial q_l}\right). \tag{62}$$

- The elastic potential energy U is given by :

$$U = \frac{1}{2} \int \bar{\bar{\sigma}} : \bar{\bar{\varepsilon}} = \frac{1}{2} q^t K q, \tag{63}$$

where $\bar{\bar{\sigma}}$ and $\bar{\bar{\varepsilon}}$ are respectively the stress and strain tensors (the colon stands for a contracted product) and K is the generalized stiffness matrix. If $\bar{\bar{\sigma_k}}$ and $\bar{\bar{\varepsilon_k}}$ are the stress and strain tensors in the basis displacement $\partial r / \partial q_k$, the (k,l)-term of K is given by :

$$K_{k,l} = \int \bar{\bar{\sigma_k}} : \bar{\bar{\varepsilon_l}}. \tag{64}$$

- The dissipated energy D is given by :

$$D = \frac{1}{2} \int f_{dis} \, . \, \dot{r}, \tag{65}$$

where f_{dis} is a dissipation force field. In most cases, this force is supposed to be viscous, which means that it is a linear function of $\dot{q}$. It is defined by :

$$f_{dis} = \sum_{i=1}^{n} \left(\frac{\partial f_{dis}}{\partial \dot{q_k}}\right) \dot{q_k} \tag{66}$$

With this hypothesis, D can be written as

$$D = \frac{1}{2} \dot{q}^t B \dot{q}, \tag{67}$$

where the generalized dissipation matrix B has its (k,l)-term given by :

$$B_{k,l} = \int \left(\frac{\partial f_{dis}}{\partial \dot{q_k}}\right) . \left(\frac{\partial r}{\partial q_l}\right) \quad . \tag{68}$$

- The matrix M is supposed definite. Like K, it is also symmetric and positive. Though B may not be symmetric, only its symmetric part has a role in (67). Writing again B for this symmetric part, it can be shown that B is positive.

• We can also consider the external forces. If f is the field of these surface forces, their work in a displacement r can be written as

$$W = \int_\Sigma r^t \, . \, f = q^t \, . \, Q \tag{69}$$

where Σ represents the structure's shape and Q is the vector of generalized forces defined by

$$Q_k = \int_\Sigma \left(\frac{\partial r}{\partial q_k}\right)^t . \, f \; . \tag{70}$$

Model equations.

• Using the principle of virtual work, rewriting (61), (63), (65) and (69) for a virtual displacement, we obtain Lagrange's equation

$$\frac{d}{dt}\left(\frac{\partial T}{\partial \dot{r}}\right) - \frac{\partial T}{\partial r} + \frac{\partial D}{\partial \dot{r}} + \frac{\partial U}{\partial r} = Q. \tag{71}$$

From the linear form of T, D, U and Q, we deduce our model equation in generalized coordinates :

$$\boxed{M\ddot{q} + B\dot{q} + Kq = Q.} \tag{72}$$

• This model equation for the movement of the structure is the most accurate model equation we can obtain with our discretization. As a matter of fact, it deals with a great number (n : dimension of the discretization) of generalized coordinates. If we suppose that the system in (72) is globally diagonalizable, we imagine that the preceding model equation handles with n structural modes. It may be more simple and efficient to limit our model equation to a fixed number of modes. In [8], Guruswamy presents the first mode shapes for a typical uniform rectangular wing. More complex modes for a simplified wing-body configuration can also be found in [8].

• We call a structural mode of (72) a displacement field U_i (with an associated pulsation ω_i) such that

$$q_i = U_i \cos(\omega_i t) \quad \text{is solution of} \quad M\ddot{q} + Kq = 0$$

which is equivalent to

$$\left(K - {\omega_i}^2 M\right) U_i = 0. \tag{73}$$

Each U_i is an eigenvector of the matrix $M^{-1}K$ with the eigenvalue ${\omega_i}^2$. Since the matrix $M^{-1}K$ is symmetric and positive, the family of displacement vectors U_i is a basis of the space of displacement fields. We can now rewrite equations (60) to (72) with U_i instead of $\partial r / \partial q_i$. Using tilded coordinates $\tilde{q}_i$ and tilded matrices and forces, we obtain

$$\tilde{M}\ddot{\tilde{q}} + \tilde{B}\dot{\tilde{q}} + \tilde{K}\tilde{q} = \tilde{Q}. \tag{74}$$

If we take for granted that all eigenvalues of M are distinct (which is the case in most studies), it can be shown that the new matrices $\tilde{M}$ and $\tilde{K}$ are both diagonal. We will write respectively (μ) and (γ) instead of $\tilde{M}$ and $\tilde{K}$. However, the matrix $\tilde{B}$ is generally not diagonal. In most cases, the hypothesis is made, that B is a linear combination of M and K (hypothesis of Rayleigh) or more simply that $\tilde{B}$ is diagonal (hypothesis of Basile) which is weaker. It has been shown [5] that Basile's hypothesis is valid for lightly-dissipative structures. For example, Borland and Rizzetta use in [4] this hypothesis with specified structural damping coefficients g_i for each mode such that

$$B = diag(g_i)\, K^{1/2}\, M^{1/2}.$$

With this new formulation and with Basile's hypothesis, writing (β) instead of $\tilde{B}$, we obtain the following modal equation, which is a set of scalar equations :

$$\boxed{(\mu)\ddot{\tilde{q}} + (\beta)\dot{\tilde{q}} + (\gamma)\tilde{q} = \tilde{Q}.} \tag{75}$$

This modal approach has been used in most available studies (see however [18] for an exception). The modal formulation allows to handle with a chosen number of variables (which are the coordinates of the displacement field on these modes). If we choose to deal with very few modes, the differential equation (75) will be solved exactly. If we choose to handle with a great amount of modes, but much less than the dimension n of the discretization, we will use the following time-integration schemes, which are much more efficient with the diagonal form (75).

4.2 Time-integration schemes.

Though the diagonal modal equation (75) could be solved exactly, a direct resolution would be too expensive in computational time. Moreover, since the general algorithm includes a rather weak simulation of the coupling between the fluid and the structure (since the structure evolves under pressure held fixed during a time step), the accuracy given by an exact resolution would be useless.

Starting from (72) and using generalized coordinates, we perform the sixth line of Table 1. Before this step, we know $P(t^{n+1})$ and $\ddot{S}(t^n)$-$\dot{S}(t^n)$-$S(t^n)$, which are respectively translated into the generalized forces $Q(t^{n+1})$ and generalized coordinates derivatives $\ddot{q}(t^n)$-$\dot{q}(t^n)$-$q(t^n)$. After this step, we must have computed the new variables $\ddot{q}(t^{n+1})$-$\dot{q}(t^{n+1})$-$q(t^{n+1})$ which will give simply $\ddot{S}(t^{n+1})$-$\dot{S}(t^{n+1})$-$S(t^{n+1})$ after another translation.

Writing q_n instead of $q(t^n)$, the scheme which is most often used takes the form :

$$\begin{cases} \dot{q}_{n+1} = \dot{q}_n + \frac{\Delta t}{2}\left(\ddot{q}_n + \ddot{q}_{n+1}\right) \\ q_{n+1} = q_n + \Delta t \dot{q}_n + \frac{\Delta t^2}{2}\left((1-\beta)\ddot{q}_n + \beta \ddot{q}_{n+1}\right) \end{cases} \tag{76}$$

and

$$M\ddot{q}_{n+1} + B\dot{q}_{n+1} + Kq_{n+1} = Q_{n+1}. \tag{77}$$

This scheme may be explained in a few words. Since we have (72) at time t^{n+1} and since we dispose of Q_{n+1}, we can use an expression of the derivatives of q at time t^{n+1} in function of one of them. The most natural choice consists in giving the leading role to the acceleration $\ddot{q}_{n+1}$ (because an error on it is reduced by time-step factors) as in (76)-(77). In the first line of the scheme (76), we have used a trapezoidal method. In the second line, we have written a hybrid method depending on a parameter β. For example, this method reduces to the trapezoidal method when $\beta = 1/2$ (see for example [18]) and to the linear acceleration method when $\beta = 1/3$ [9].

The global time-integration algorithm takes the final computational form of the five following steps :

$$\circ \quad \dot{q}_* = \dot{q}_n + \frac{\Delta t}{2}\ddot{q}_n \tag{78}$$

$$\circ \quad q_* = q_n + \Delta t\, \dot{q}_n + \frac{\Delta t^2}{2}(1-\beta)\ddot{q}_n \tag{79}$$

- ○ $$\ddot{q}_{n+1} = \left[M + \frac{\Delta t}{2} B + \beta \frac{\Delta t^2}{2} K \right]^{-1} (Q_{n+1} - B\dot{q}_* - Kq_*) \tag{80}$$
- ○ $$\dot{q}_{n+1} = \dot{q}_* + \frac{\Delta t}{2} \ddot{q}_{n+1} \tag{81}$$
- ○ $$q_{n+1} = q_* + \beta \frac{\Delta t^2}{2} \ddot{q}_{n+1} \tag{82}$$

This algorithm is actually general. We could have written the corresponding algorithm with modal matrices, forces and coordinates. In that case, the most expensive step written in (80) would have been much more cheaper because $\tilde{M}$, $\tilde{B}$ and $\tilde{K}$ are diagonal.

We see here the most important advantage of the modal formulation. The computations of the structural modes and the modal mass, damping and stiffness matrices are made once and for all. The time-integration algorithm is thereafter very efficient, since no complex computations are performed during each time step. After each step, it is however necessary to compute the position and the speed of the structure, written S^{n+1} and $\dot{S}^{n+1}$ in the preceding section. These variables are actually used in the aerodynamic part of the general algorithm. They may be obtained with help of the fixed transformation matrix from $\partial r / \partial q_i$ to U_i.

In short, the structural dynamics phase on line 6 of Table 1 is quite cheap for each time step when modal equations are used. Several tasks must be accomplished for each time step. First, a translation of pressure forces at the current step and dynamic characteristics of the structure at the previous step into generalized coordinates is performed. Second, the scheme (78) to (82) (the most difficult step is the inversion of a diagonal matrix) gives new generalized coordinates for the displacements. Finally, another translation of these coordinates into dynamic characteristics of the structure at the end of the step is necessary.

The computations performed once and for all are the calculations of generalized matrices M, B and K, the diagonalization of $M^{-1}K$, the saving of a chosen number of eigenvectors and of the diagonal matrices (μ), (β) and (γ). Last but not least, transfer matrices from generalized to modal and modal to generalized coordinates must be computed and saved.

References

[1] W.K. ANDERSON, J.L. THOMAS & C.L. RUMSEY, "Extension and Application to Unsteady Calculations on Dynamic Meshes", *AIAA paper* N^0 87-1152, AIAA Eighth Computational Fluid Dynamics Conference, Honolulu, Hawaii, June 9–11 (1987).

[2] J.T. BATINA, "Unsteady Euler Airfoil Solutions Using Unstructured Dynamic Meshes", *AIAA Journal*, vol.28, Aug., pp 1381–1388 (1990).

[3] J.T. BATINA, "Implicit Flux-Split Euler Schemes for Unsteady Aerodynamic Analysis Involving Unstructured Dynamic Meshes", *AAIA Journal*, vol.29, Nov., pp 1836–1843 (1991).

[4] C.J. BORLAND & D.P.RIZZETTA, "Nonlinear Transonic Flutter Analysis", *AIAA Journal*, vol.20, Nov., pp 1606–1615 (1982).

[5] R. DAT, "Vibrations aéroélastiques", *ENSAE*, Cours de l'Ecole Nationale Supérieure de l'Aéronautique et de l'espace, Département des Structures-Matériaux-Technologie (1978).

[6] J. DONEA, P. FASOLI-STELLA & S. GIULIANI, "Finite element solution of transient fluid-structure problems in Lagrangian coordinates", *Proc. Int. Meeting on Fast Reactor Safety and Related Physics*, vol.III, Chicago, pp 1427–1435 (1976).

[7] J. DONEA, S. GIULIANI & J.P. HALLEUX, "An Arbitrary Lagrangian Eulerian Finite Element Method for Transient Dynamic Fluid-Structure Interactions", *Computer Methods in Applied Mechanics and Engineering*, vol.33, pp689–723 (1982).

[8] G.P. GURUSWAMY, "Interaction of Fluids and Structures for Aircraft Applications", *Computers & Structures*, Vol.30, N^0 1/2, pp 1–13 (1988).

[9] G.P. GURUSWAMY, "Unsteady Aerodynamic and Aeroelastic Calculations for Wings Using Euler Equations", *AIAA Journal*, vol.28, Mar., pp 461–469 (1990).

[10] G.P. GURUSWAMY, "Integrated Approach for Active Coupling of Structures and Fluids", *AIAA Journal*, vol.27, Jun., pp 788–793 (1989).

[11] G.P. GURUSWAMY, "Vortical Flow Computations on Swept Flexible Wings Using Navier-Stocks Equations", *AIAA Journal*, vol.28, Dec., pp 2077–2084 (1990).

[12] A. HARTEN & J.M. HYMAN, "Self Adjusting Grid Methods for One-Dimensional Hyperbolic Conservation Laws", *Journal of Computational Physics*, vol.50, pp 235–269 (1983).

[13] K. ISOGAI & K. SUETSUGU, "Numerical Calculation of Unsteady Transonic Potential Flow over Three-Dimensional Wings with Oscillating Control Surfaces", *AIAA Journal*, vol.22, Apr., pp 478–485 (1984).

[14] O.A. KANDIL & H.A. CHUANG, "Unsteady Transonic Airfoil Computation using Implicit Euler Scheme on Body-fixed Grid", *AIAA Journal*, vol.27, Aug., pp 1031–1038 (1989).

[15] S. LANTERI, "Simulation d'Ecoulements Aérodynamiques Instationnaires sur une Architecture S.I.M.D. Massivement Parallèle", *Ph.D. Thesis*, Sciences de l'Ingénieur, Université de Nice-Sophia-Antiplois, France (1991).

[16] K.J. LIN, P.J. LU & J.Q.TARN, "Flutter Analysis of Cantilever Composite Plates in Subsonic Flow", *AIAA Journal*, vol.27, Aug., pp 1102–1109 (1989).

[17] T.Y. LIN, "A multiple frames of reference approach to aeroelastic computations : application to airfoil flutter analysis", *Ph.D. Thesis*, Department of Aerospace Engineering Sciences, University of Colorado, Boulder, Colorado (1990).

[18] T.Y. LIN, "Transient Aeroelastic Computations Using Multiple Moving Frames of Reference", *AIAA paper* N^0 90-3053-CP (1990).

[19] R. LOHNER, "An Adaptive Finite Element Solver for Transient Problems with Moving Bodies", *Computers & Structures*, Vol.30, N^0 1/2, pp 303–317 (1988).

[20] I. LOTTATI, "The Role of Structural and Aerodynamic Damping on the Aeroelastic Behavior of Wings", *Journal of Aircraft*, vol.23, Jul., Engineering notes, pp 606–608 (1986).

[21] D.J. MAVRIPLIS, "Multigrid Solution of the Two-Dimensional Euler Equations on Unstructured Triangular Meshes", *AIAA Journal*, vol.26, Jul., pp824–831 (1988).

[22] K. NAKAHASHI & G.S. DEIWERT, "Self-adaptive Grid Method with Application to Airfoil Flows", *AIAA Journal*, vol.25, Apr., pp 513–520 (1987).

[23] B. N'KONGA & H. GUILLARD, "A Roe Scheme on Non-Structured Meshes for Moving Boundaries Problems", *Proceedings of the 13th IMACS World Congress on Computational and Applied Mathematics*, Trinity College, Dublin, Ireland, July 22-26, vol.1, pp 447–449 (1991).

[24] S. OBAYASHI, G.P. GURUSWAMY & P.M. GOORJIAN, "Streamwise Upwind Algorithm for Computing Unsteady Transonic Flows Past Oscillating Wings", *AIAA Journal*, vol.29. Oct., pp 1668–1677 (1991).

[25] K.C. PARK, C.A. FELIPPA & J.A. DE RUNTZ, "Stabilization of Staggered Solution Procedures for Fluid-Structure Interaction analysis", in T. Belytschko and T.L. Geers (eds), Computational methods for fluid-structure interaction problems (ASME Applied Mechanics Symposia Series, AMD-vol.26, pp 94–124 (1977).

[26] B.S. SARMA & T.K. VARADAN, "Nonlinear Panel Flutter by Finite-Element Method", *AIAA Journal*, vol.26, May, pp 566–574 (1988).

[27] R.H. SCANLAN, "On the State of Stability Considerations for suspended-span bridges under Wind", *Proceedings IUTAM-IAHR Symposium*, Karlsruhe, Germany, pp 595–618 (1979).

[28] V. SHANKAR & H. IDE, "Aeroelastic computations of flexible configurations", *Computers& Structures*, vol.30, N^0 1/2, pp 15–28 (1988).

[29] P.D. THOMAS & C.K. LOMBARD, "Geometric Conservation Law and Its Application to Flow Computations on Moving Grids", *AIAA Journal*, vol.17, Oct., pp 1030–1037 (1979).

Contents